Diffusion and structure in silica liquid: a molecular dynamics simulation

2007 J. Phys.: Condens. Matter 19 466103

(http://iopscience.iop.org/0953-8984/19/46/466103)

IOP PUBLISHING JOURNAL OF PHYSICS: CONDENSED MATTER

J. Phys.: Condens. Matter **19** (2007) 466103 (12pp) doi:10.1088/0953-8984/19/46/466103

Diffusion and structure in silica liquid: a molecular dynamics simulation

P K Hung, N V Hong and L T Vinh

Department of Computational Physics, Hanoi University of Technology, Vietnam, 1 Dai Co Viet, Hanoi, Vietnam

E-mail: pkhung@fpt.vn

Received 4 April 2007, in final form 21 August 2007
Published 10 October 2007
Online at stacks.iop.org/JPhysCM/19/466103

Abstract

Diffusion and structure in liquid silica under pressure have been investigated by a molecular dynamics model of 999 atoms with the inter-atomic potentials of van Beest, Kramer and van Santen. The simulation reveals that silica liquid is composed of the species SiO_4, SiO_5 and SiO_6 with a fraction dependent on pressure. The density as well as volume of voids can be expressed as a linear function of the fraction of those species. Low-density liquid is mainly constructed of SiO_4 and has a large number of O- and Si-voids and a large void tube. This tube contains most O-voids and is spread over the whole system. The anomalous diffusion behavior is observed and discussed.

1. Introduction

The structure and diffusion of ions in liquid silica has been under intensive study from both experiment and computer simulation [1–12]. One of the major successes in molecular dynamics (MD) simulation is Waff's prediction stating that the self-diffusion coefficient (SDC) of network-forming species increases with pressure [1]. Later, this effect was verified by experiments [2] and by MD works on silica and alkali silicate [3, 4, 9], suggesting that the SDCs of Si and O increase with pressure and reach a maximum around 12–15 GPa [3]. The temperature dependence of SDCs in liquid SiO_2 is studied in [3, 33] which finds that SDCs show the Arrhenius law at low temperature and the power law at high temperature. Furthermore, their calculated activation energies for diffusion of Si and O are very close to the experimental data in [5, 6] (its values for Si and O are 6 and 4.7 eV respectively). Recently, the anomalous diffusion and structural order in silica liquid have been studied in MD models [8]. According to the result from [8], at a density of 3000 kg m^{-3}, the dynamics become faster due to the disruption of structural order, but at a density of 4000 kg m^{-3} the dynamics are slow due to the high density. We also find some other works concerning the anomalous diffusion in liquids such as SiO_2, GeO_2 and H_2O [11, 13–17]. However, most models interpreted this phenomena as relatively simple, based mainly on the coordination analysis.

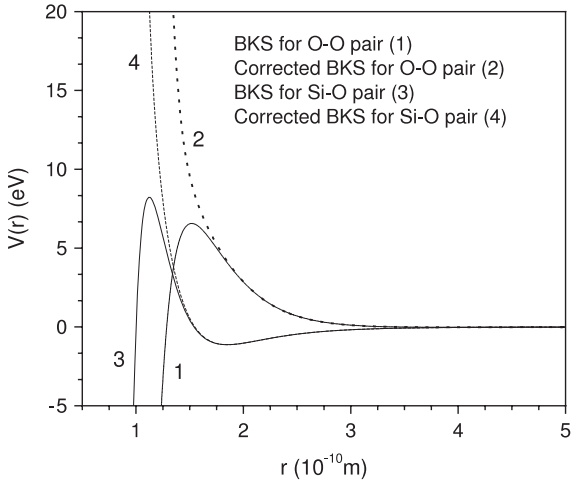

Figure 1. The BKS and corrected BKS potentials.

First-principle simulation can provide very accurate data for numerous physical properties of silica liquid and glass [27, 28], but it is limited to a few hundred atoms at most. Hence, the classical MD simulation is an effective way to deal with such problems where the long- or intermediate-range order is involved [33–35]. In particular, as shown in [21, 27, 29, 33–35] classical force fields are indeed able to give a good description of quantities like the structural factor, viscosity and diffusion constants. The characteristic feature of network-forming fluids is the presence of a large number of voids [18–20, 22, 23]. Despite the fact that voids are strongly related to diffusion and densification, the void as well as its aggregation in liquid SiO_2 under pressure has not yet been investigated. Therefore, the goal of current work is to show voids and their role for diffusion and densification in simulated liquid SiO_2. In addition, we determined whether the basic units SiO_x ($x = 4, 5$ and 6) are identical in constructed MD models under different pressure and the relationship between the SiO_x fraction and some physical properties is clarified. These issues, to our knowledge, have not been addressed in earlier MD studies of pressure-induced liquids SiO_2 [11, 17, 28, 29, 33–35]. We also interpret the microscopic mechanism of densification and of dynamics in liquid SiO_2, based on the viewpoint that liquid is a mixture of species SiO_x with the fraction varied with pressure.

2. Calculation method

We conduct the MD simulations for a system of $N = 999$ atoms (666 O and 333 Si). The van Beest, Kramer, van Santen (BKS) potential is adopted [24] because it is still simple and produces well structural and dynamic properties for liquid SiO_2 [7, 8]. The Ewald summation is used to calculate the long-range Coulomb interactions. The BKS potential has the non-physical feature that the interaction energy for the Si–O pairs diverges to $-\infty$ as their separation goes to zero, so we add a Lennard-Jones (15-6 type) term to the BKS potential that prevents this effect at short distance, but it does not alter the form of the BKS potential at large separation. In figure 1 we compare the corrected BKS potential with its original form. It can be seen that both curves almost coincide with each other at atomic separation larger than 1.9 Å. The MD time step is equal to 0.4 fs. It is essential to notice that the accuracy of the MD method depends on the value of MD time step used in the simulation. Commonly, it is taken to be about 1 fs, which

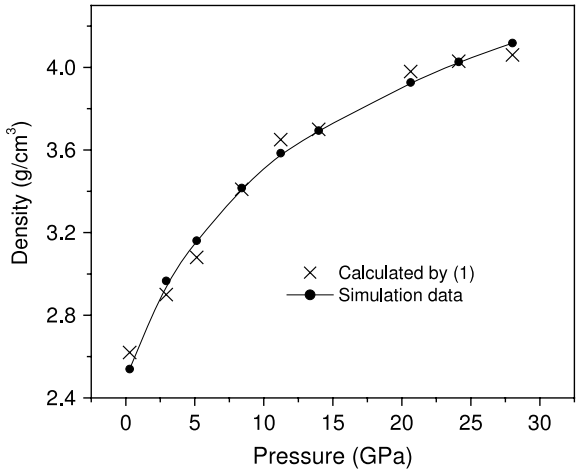

Figure 2. Density versus pressure for silica liquid at 3000 K.

is twice as large as the MD time step used in our work. In our experience this MD time step allows us to get high accuracy in calculation. The initial configuration is a good equilibrium model of liquid SiO_2 at 3000 K and at ambient pressure. This model has been prepared by the method described in detail in [19]. For each state point, the simulation is conducted upon constant pressure and temperature (NPT ensemble) and the system is equilibrated to near 3000 K and the desired pressure P. Then the system is held upon constant volume and energy (NVE ensemble) within 200 000 MD steps to reach a good equilibrium. For each run, the pair radial distribution function and thermodynamic quantity (P, V, T, E) of the system are examined many times to check whether the system reaches the equilibrium state. After that we calculate the positional and angular characteristics by averaging over the 1000 last configurations separated by 10 MD steps.

If every atom is considered as a sphere, then there is a part of the model in which no atomic sphere lies. The radii of Si and O atoms is 1.46 and 0.73 Å respectively. The void is defined as a sphere that is in contact with four atoms and does not intersect with any atom. Details of the void calculation can be found elsewhere [18, 19].

3. Result and discussion

3.1. Local structure

An overview of our simulations is presented in figure 2, which displays the plot of density versus pressure. The structural characteristics of the constructed models is summarized in table 1. It can be seen that the BKS model at ambient pressure reproduces well the structural data obtained experimentally. Now we turn our attention to building blocks (basic units) SiO_x and it is necessary to determine the distribution of silicon coordination number (CN). To calculate CN we used the cutoff distance, chosen as a minimum after the first peak in the pair radial distribution functions (PRDF). The cutoff distance is determined by averaging over the 1000 last configurations separated by 10 MD steps. The error of the calculated cutoff distance is ± 0.02 Å. Figure 3 shows the dependence of SiO_x fractions on pressure. Here $x = 4$, 5 and 6. We also find some SiO_x with $x = 3$, 7 and 8, but their fraction is smaller than 0.01. The fraction of four-coordinated silicon decreases by 39% as pressure increases from 0.28 to

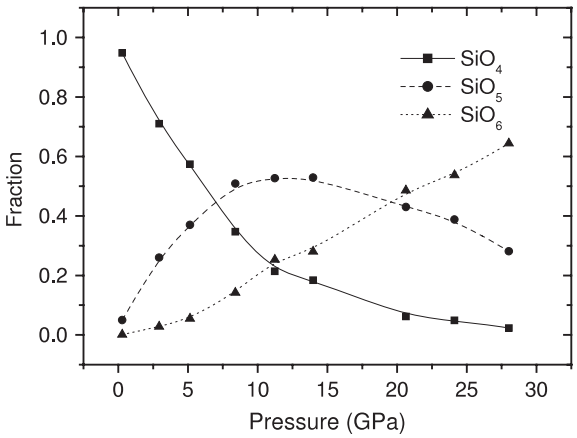

Figure 3. The dependence of SiO_4, SiO_5 and SiO_6 fractions on pressure for silica liquid at 3000 K.

Table 1. Structural characteristics of silica liquid at 3000 K. r_{ij}, g_{ij}—the position and height of the first peak in PRDFs $g_{ij}(r)$; Z_{ij}—the averaged coordination number. Here 1–1 for the Si–Si pair; 1–2 for the Si–O; 2–1 for the O–Si; 2–2 for the O–O.

	r_{ij} (Å)			g_{ij}			Z_{ij}			
Pressure (GPa)	1–1	1–2	2–2	1–1	1–2	2–2	1–1	1–2	2–1	2–2
0.28	3.10	1.60	2.60	3.12	10.23	2.91	4.34	4.05	2.02	7.96
2.93	3.10	1.60	2.60	2.73	8.33	2.61	5.16	4.31	2.16	11.42
5.14	3.10	1.60	2.56	2.61	7.52	2.52	5.78	4.48	2.24	12.10
8.40	3.08	1.62	2.52	2.48	6.55	2.44	6.95	4.79	2.40	13.24
11.23	3.10	1.62	2.50	2.48	6.10	2.45	7.50	5.05	2.53	14.01
13.98	3.08	1.62	2.50	2.47	5.97	2.45	8.01	5.11	2.55	14.35
20.64	3.10	1.64	2.46	2.50	5.58	2.53	8.67	5.47	2.73	15.15
24.12	3.10	1.64	2.46	2.44	5.50	2.54	8.97	5.54	2.77	15.75
28.02	3.08	1.64	2.46	2.49	5.49	2.58	8.92	5.72	2.86	15.66
0[a]	3.12	1.62	2.65							
0[b]	3.077	1.608	2.626							

[a] Experimental data from [30].
[b] Experimental data from [31, 32].

5.14 GPa. In this pressure region most of the loss of SiO_4 is accounted for by an increase in SiO_5. With further increasing pressure, SiO_6 gradually replaces the SiO_4 and SiO_5. Beyond 29 GPa the percentage of six-coordinated silicon reaches about 65% and it clearly indicates the transformation of liquid silica from tetrahedral to octahedral network structure.

Useful information about SiO_x can be inferred from the bond-angle distributions. In this work we only calculate the most important angles such as the O–Si–O and Si–O–Si angles. The fist angle characterizes the atomic arrangement inside SiO_x and the second one provides the connectivity between them. In figure 4 we display the angle distributions calculated separately for SiO_4, SiO_5 and SiO_6 units. For the ideal tetrahedron SiO_4 the angle of O–Si–O is equal to 109.7°. Therefore, a maximum at 105° for an O–Si–O angle distribution of SiO_4 indicates the distorted tetrahedral network structure. In the case of SiO_5 and SiO_6 we observe two peaks centered at 90° and 155°. It is interesting to note that the O–Si–O angle distributions are almost unchanged with pressure (see figure 4). The Si–O bond-length also changes little under

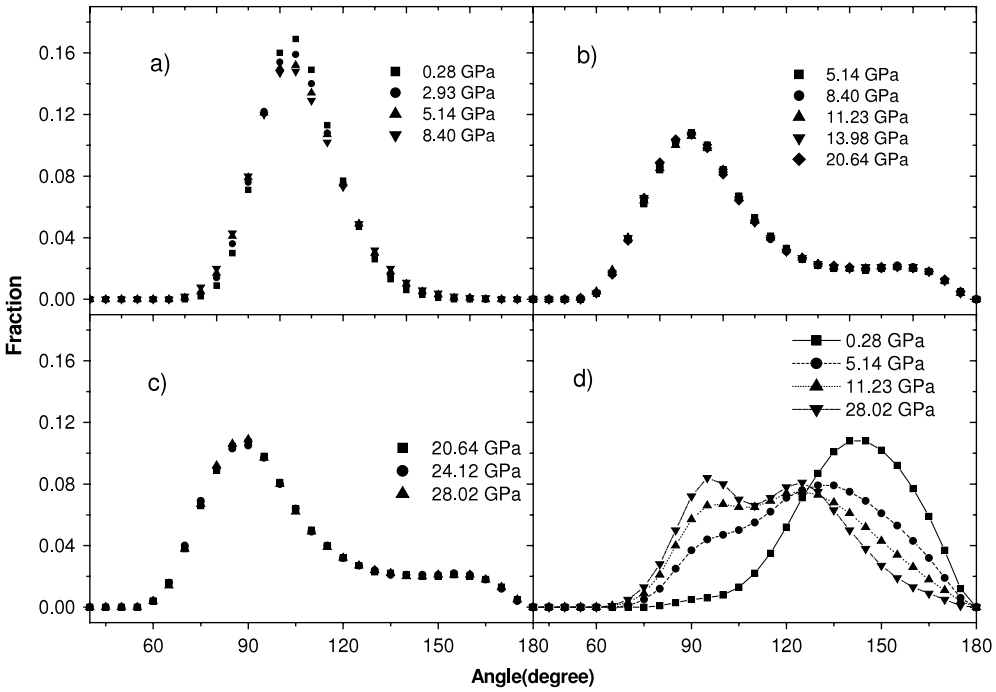

Figure 4. The angle distribution for silica liquid at 3000 K. (a) for O–Si–O in SiO_4; (b) for O–Si–O in SiO_5; (c) for O–Si–O in SiO_6 and (d) for Si–O–Si.

pressure. It means that the units SiO_x are identical in different simulated liquids; hence we can conclude that silica liquid likes a mixture of species SiO_4, SiO_5 and SiO_6 with the proportions varied with pressure. A two-state model in which the liquids are assumed to be made up of low- and high-density species, successfully describes the polymorphism for such liquids as SiO_2 and GeO_2 [10, 12]. In accordance with our simulation, these species are SiO_4, SiO_5 and SiO_6; and their proportions vary with pressure. From this viewpoint one can expect that some physical properties of silica liquid could be expressed as a function of SiO_4, SiO_5 and SiO_6 fractions. Thereby, the density of system ρ can be given as

$$\rho = aC_{SiO_4} + bC_{SiO_5} + cC_{SiO_6}, \tag{1}$$

where C_{SiO_4}, C_{SiO_5}, C_{SiO_6} are the fraction of SiO_4, SiO_5 and SiO_6 given from figure 3; a, b and c are parameters equal to 2.564, 3.666 and 4.614 g cm^{-3} GPa^{-1}, respectively. As shown from figure 1, the calculated data from the simulation and (1) are in excellent agreement.

The valuable information about linkage between two adjacent SiO_x is provided by the Si–O–Si angle and the distribution of oxygen linkage. As shown from figure 4, at low pressure the Si–O–Si angle distribution has a main peak at 144° and it is closed to experimental data [25, 26]. At higher pressure the Si–O–Si angle distributions split into two peaks. These peaks are located at 95° and 125° at 28.04 GPa. Two adjacent SiO_x are linked to each other through common oxygen, which we denote as 'bridge oxygen'. The distribution of oxygen linkages is presented in table 2. According to this table, most connections are one-oxygen, but as the pressure increases, the fraction of two- and three-oxygen connectivity becomes considerable, which reflects on the appearance of two peaks in figure 4(d).

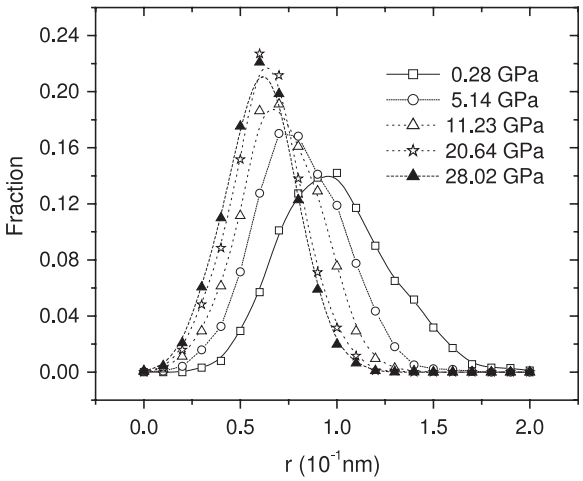

Figure 5. The radii distribution of voids.

Table 2. The distribution of oxygen linkages. m is the number of oxygens that two neighbor units SiO_x are bonded to. The next columns indicate the percentage of connectivity. For example, at 0.28 GPa, 1.21% of connectivity is two-oxygen.

	Pressure (GPa)								
m	0.28	2.93	5.14	8.40	11.23	13.98	20.64	24.12	28.02
1	98.77	92.58	88.80	84.07	80.90	78.96	76.44	75.67	74.04
2	1.21	7.24	10.70	14.95	17.80	19.59	21.73	21.82	23.44
3	0.01	0.18	0.50	0.98	1.30	1.45	1.83	2.51	2.51
4	0.00	0.00	0.00	0.00	0.00	0.00	0.00	0.00	0.01

3.2. Void and void aggregation

Figure 5 shows the void radii distribution (VRD). The major change with increasing pressure observed here is a shifting of the main peak to small radii and the VRD becoming broader as pressure lowers. In the pressure range from 0.28 to 5.14 GPa, the peak of the VRD shifts from 1 to 0.7 Å and its height increases from 0.14 to 0.17 respectively. With further increasing pressure the position of the VRD peak remains unchanged, but its height gradually increases. In the pressure region of 20.64–28.02 GPa the VRD is almost unchanged.

As mentioned above, voids could locate next to each other and create a large cluster. In the current work we examined two kinds of void aggregations: void cluster (VC) and void tube (VT). The first void aggregation is a set of voids consisting of a central void and several smaller voids overlapping the central void. The second one contains a number of voids with radius bigger than the radius of an oxygen atom and each void in a VT must overlap at least with an adjacent void by a section circle with a radius bigger than the oxygen radius. From a geometric viewpoint, the VT is a channel along which the oxygen can travel without intersection with any atomic sphere. Some typical VC and VT clusters detected in our models are shown in figure 6.

In order to gain more detail about a VC we also calculate its volume by randomly generating several thousand points in a cube containing a VC. The volume of a VC is calculated as: $V_{\mathrm{VC}} = V_{\mathrm{cube}} \cdot n_{\mathrm{in}}/n_{\mathrm{total}}$. Here V_{cube} is the volume of the cube; n_{total} is the total number of generating points, n_{in} is the number of points located within VC. The VC volume distributions

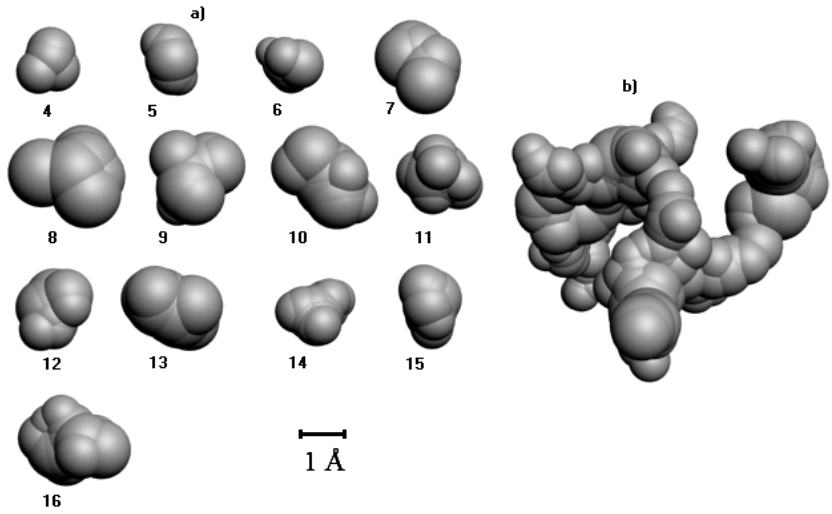

Figure 6. The VC (a) and VT (b); the number below the VC image shows the number of voids in this VC.

Table 3. The volume distribution of VCs. The first column shows the volume range. Numbers 0, 1, 2, 3 and 4 in the first column correspond to the volume range of: 0–13.04 Å^3; 13.04–26.08 Å^3; 26.08–39.12 Å^3 and bigger than 39.12 Å^3. The next column indicates the number of VCs detected in the model. For example, at 2.93 GPa there are 95 VCs with volumes in the range of 13.04–26.08 Å^3.

	Pressure (GPa)								
	0.28	2.93	5.14	8.4	11.23	13.98	20.64	24.12	28.02
0	768	1028	1190	1228	1335	1378	1460	1487	1507
1	115	95	75	53	25	25	8	7	4
2	36	14	5	3	1	0	0	0	0
3	17	2	2	0	0	0	0	0	0
4	6	0	0	0	0	0	0	0	0

are presented in table 3. From this table we can see that the number of voids with volume bigger than 13.04 Å^3 (volume of silicon $= 4\pi r_{\mathrm{Si}}^3/3 = 13.04$ Å^3; r_{Si} is the radius of silicon) monotonically decreases with pressure. Meanwhile, in contrast, the number of VCs with smaller volume increases. At ambient pressure we find six very big VCs with volume at least four times bigger than the volume of a silicon atom. Obviously, these VCs like the microscopic cavity.

Table 4 shows that the number of VCs and VTs increases by 1.6 times and 2.1 times, respectively, as pressure increases from 0.28 to 28.02 GPa. Among the VTs in each system we denote the largest one as LVT. Under a pressure of 0.28 GPa the LVT contains 3033 voids, which is 91% of voids with radius bigger than the oxygen radius. Hereafter, we call this void the O-void and a void with radius bigger than the silicon radius the Si-void. With increasing pressure the number of O-voids in LVTs rapidly decreases. Accordingly, at 28.02 GPa the LVTs have only 28 O-voids which is about 2% of the O-voids. To estimate the evolution of void and void aggregation, we calculated the ratio between the volume occupied by voids and the volume of the simulation cell. Figure 7 displays the volume fraction of various kinds of

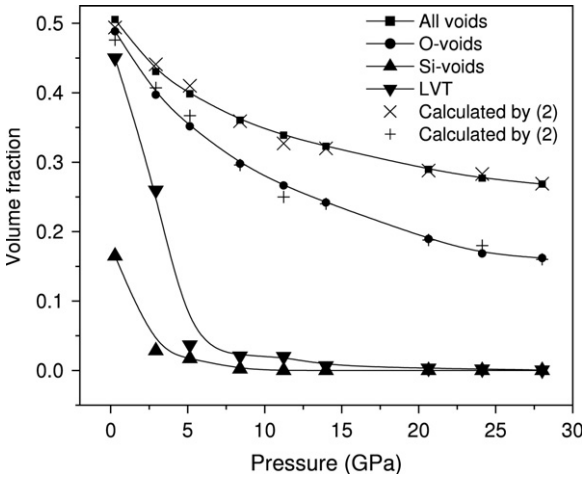

Figure 7. The dependence of volume fraction on pressure.

Table 4. The characteristics of VCs and VTs. N_{VC}, N_{VT} are the number of VCs and VTs; N_{LVT} is number of voids in LVTs.

	Pressure (GPa)								
	0.28	2.93	5.14	8.4	11.23	13.98	20.64	24.12	28.02
N_{VC}	942	1139	1272	1284	1361	1403	1468	1494	1511
N_{VT}	146	249	306	307	341	316	349	313	307
N_{LVT}	3033	2033	292	182	202	62	38	37	28

voids versus pressure. We can see that they are close to each other at low pressure, but under higher pressure, the volume fraction of Si-voids and LVTs rapidly decreases to zero. As in the case of density, the volume fraction of all voids and O-voids is a linear function of the fraction of SiO_4, SiO_5 and SiO_6 as follows:

$$\upsilon_v = a_v C_{SiO_4} + b_v C_{SiO_5} + c_v C_{SiO_6}. \tag{2}$$

Here $a_v = 0.506$; $b_v = 0.283$; $c_v = 0.277$ for all voids and $a_v = 0.491$; $b_v = 0.208$; $c_v = 0.140$ for O-voids. The data calculated by (2) is presented in figure 7 and we observed again a good agreement.

It is interesting to compare the ΔV and the decrease in volume occupied by various kinds of voids under densification. Here ΔV is the decrease in volume of the simulation cell. The result of this calculation is shown in figure 8 and we can see that ΔV is close to the decrease in the volume occupied by all voids. Therefore, the part of the simulation cell occupied by silicon and oxygen atoms is almost unchanged during densification. Furthermore, the horizontal lines in figure 8 indicate that as the pressure becomes higher than 8.4 GPa most Si-voids as well as the major part of the LVTs were eliminated.

We now analyse the microscopic mechanism responsible for the large compressibility of liquid silica. The author in [28] stated that the coordination changes are not sufficient alone to explain the compressibility of liquid SiO_2 and three different mechanisms must occur: (1) reduction of the Si–Si distance, (2) elimination of three-member rings and (3) an increase in connectivity caused by coordination defects. Another mechanism (the continuous restructuring) is proposed in [35], suggesting the local breaking and reconnecting of bonds.

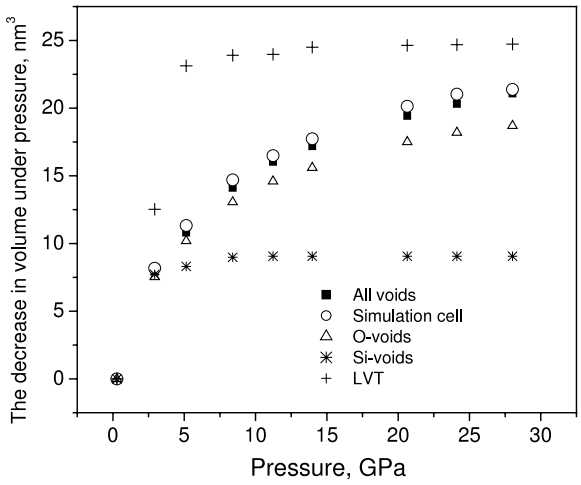

Figure 8. The decrease in volume of voids and void aggregation under pressure.

Overall, from these works it is not clear what the quantitative contribution of the above-mentioned mechanism in volume reduction is. Our simulation reveals that the change in fraction of SiO_4, SiO_5 and SiO_6 is responsible for densification and the replacing of SiO_4 by SiO_6 or SiO_5 is accompanied with a significant decrease in the volume of voids. It also means that the densification involves the change in number of various kinds of SiO_x existing in the system. In particular, each SiO_6 and SiO_5 contributed 1.8 and 1.43 times the volume reduction with respect to SiO_4 (see parameters a, b and c in equation (1)); the volume of all voids was reduced by up to 50% between 0 to 28.02 GPa (see figures 7 and 8). It is interesting to note that the quartz/stishovite density ratio is 1.3 which is quite alot smaller than the SiO_6/SiO_4 volume contribution obtained in our simulation ($\sim$1.8). This large difference is caused by voids located between SiO_x; those voids became significantly smaller under high pressure. Therefore, the discrepancy between our simulation and the result in [28, 35] is that these authors use the quartz/stishovite density ratio to estimate the compressibility and different inter-atomic potentials are used in our work and their work.

3.3. Diffusion

The diffusion coefficient for components in a system can be calculated as

$$\lim_{t\to\infty} \frac{\langle r^2(t)\rangle}{6t} = D, \tag{3}$$

where $\langle r(t)^2\rangle$ is the mean-squared displacement of atoms which is plotted in figure 9. The result for diffusion constants D_x are shown in figure 10. Here the anomalous variation of the diffusion constant is observed with a maximum around 10–12 GPa. The non-monotonous behavior D_x is already reported in [8, 29] (with different model). Furthermore, the coefficient D_{Si} is close to D_O at ambient pressure and at 28.02 GPa, but at around 10–12 GPa D_O became larger than D_{Si}. This result can be interpreted based on the above-mentioned viewpoint that liquid silica is composed of species SiO_4, SiO_5 and SiO_6. Because the ratio D_{Si}/D_O is close to 1, the oxygen and silicon probably diffuse by movement of species SiO_x. In accordance with figure 2 we can notice that the maximum of fraction SiO_5 in the investigated pressure range is reached at around 10–12 GPa, corresponding to the maximum shown in figure 10. It means that the

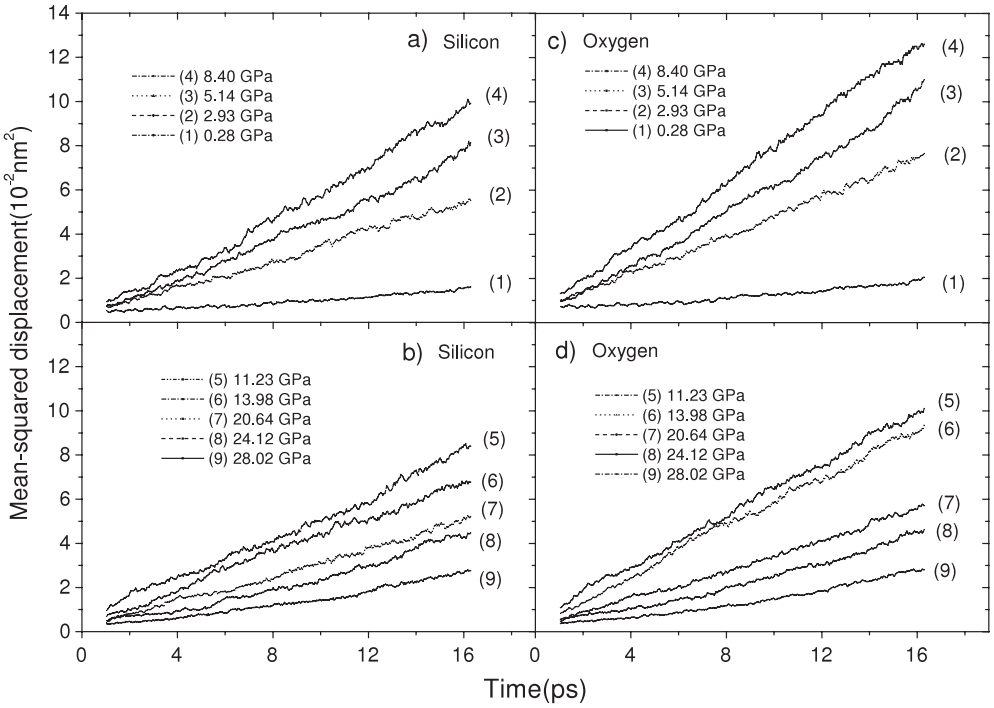

Figure 9. Mean-squared displacement versus time for Si ((a), (b)) and O ((c), (d)) atoms.

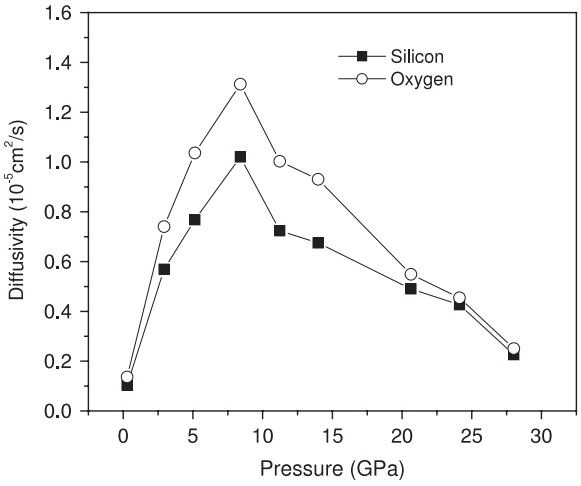

Figure 10. The diffusion constants versus pressure.

mobility of SiO_5 is much faster than SiO_4 and SiO_6. Correspondingly, as pressure increases to 10–12 GPa both D_{Si} and the fraction of SiO_5 increases. Further increasing the pressure results in decreasing D_{Si} and the fraction of SiO_5, but at 28.02 GPa the D_{Si} is still greater than that at ambient pressure. Because the fraction of SiO_6 is dominant at 28.02 GPa, whereas the majority of SiO_x is SiO_4 at ambient pressure, the mobility of SiO_6 is greater than that of SiO_4.

We now turn our attention to the diffusion mechanism of oxygen. Figure 10 clearly indicates the change in diffusion mechanism for silicon and oxygen between 0 and 10–12 GPa. The existence of LVTs, VCs and a large number of O-voids ensures the possibility of oxygen diffusion via O-voids through LVTs and VCs as non-bonding oxygen. However, at ambient pressure this mechanism is excluded due to strong Si–O bonds in SiO_4 and the system contains only SiO_4. As pressure increases to 10–12 GPa the fraction SiO_5 is dominant and the size of LVTs is also large enough. Moreover, the two- and three-oxygen connectivity becomes considerable, which favors the oxygen breaking Si–O bonds and diffusing via O-voids. It then leads to a considerable contribution of oxygen hopping via O-voids in comparison with the movement of species SiO_x. We also observed that the diffusion constant D_O is larger than D_{Si}.

Further increasing the pressure results in the elimination of O- and Si-voids. The LVTs become too small, which prevents oxygen diffusion by the hopping mechanism and we observe again the ratio $D_{Si}/D_O \sim 1$ as in the case of ambient pressure. This means that Si and O diffuse mainly through the movement of SiO_5 and SiO_6.

4. Conclusions

The main conclusions that can be drawn are as follows.

(i) The MD simulation shows that the silica liquid is made up of a mixture of species SiO_4, SiO_5 and SiO_6. For the first time we find that these species are identical in different constructed models, therefore pressure-induced liquid silica is like a mixture of those species with the fraction varied with pressure. This issue is supported by the fact that some physical properties, such as the density and volume of voids, could be expressed as a linear function of SiO_4, SiO_5 and SiO_6 fractions. Low-density liquid (low pressure) is constructed mainly by SiO_4 and has a large number of O-voids, Si-voids and a large LVT. This LVT contains most O-voids and is spread over the whole system. Furthermore, low-density liquid also contains many microscopic cavities (large VCs). In contrast, for a high-density liquid the number of O-voids, Si-voids as well as the size of LVTs is much smaller than in a low-density liquid. The densification concerns mainly the elimination of voids, but the part of the simulation cell occupied by oxygen and silicon is almost unchanged. The structure of the low-density liquid also differs from the high-density liquid in the distribution of oxygen linkages.

(ii) We find that the diffusion mechanism of oxygen is changed under pressure. Correspondingly, the oxygen and silicon probably diffuse by the movement of SiO_x at 0 and at 28.02 GPa. Oxygen starts to diffuse by the hopping mechanism via O-voids through LVTs and VCs around 10–12 GPa. The mobility of SiO_5 is much greater than that of SiO_4 and SiO_6.

References

[1] Waff H S 1975 *Geophys. Res. Lett.* **2** 193
[2] Woodcock L V, Angell C A and Cheeseman P 1976 *J. Chem. Phys.* **65** 1565
[3] Kushiro I 1976 *J. Geophys. Res.* **81** 6347
[4] Rustad J R, Yuen D A and Spera F J 1990 *Phys. Rev.* A **42** 2081
[5] Brebec G, Seguin R, Sella C, Bevenot J and Martin J C 1980 *Acta Metall.* **28** 327
[6] Mikkelsen J C 1984 *Appl. Phys. Lett.* **45** 1187
[7] Horbach J and Kob W 1999 *Phys. Rev.* B **60** 3169
[8] Scott Shell M, Debenedetti P G and Panagiotopoulos A Z 2002 *Phys. Rev.* E **66** 011202
[9] Morishita T 2005 *Phys. Rev.* E **72** 021201

[10] Voivod I S, Sciortino F and Poole P H 2000 *Phys. Rev.* E **63** 3182
[11] Hoang V V, Zung H and Hai N T 2007 *J. Phys.: Condens. Matter* **18** 116104
[12] Wolf G H and McMillan P F 1995 *Structure, Dynamics and Properties of Silicate Melts* (*Rev. Mineral.* vol 32) ed J F Stebbins, P F McMillan and D B Dingwell (Washington, DC: Mineralogical Society of America) pp 505–61
[13] Starr F W, Sciortino F and Stanley H E 1999 *Phys. Rev.* E **60** 6757
[14] Starr F W, Harrington S, Sciortino F and Stanley H E 1999 *Phys. Rev. Lett.* **82** 3629
[15] Errington J R and Debenedetti P G 2001 *Nature* **409** 318
[16] Tsuneyuki S and Matsui Y 1995 *Phys. Rev. Lett.* **74** 3197
[17] Hoang V V, Huynh N, Anh T and Zung H 2007 *Physica* B **390** 17
[18] Hung P K, Hue H V and Vinh L V 2006 *J. Non-Cryst. Solids* **352** 3332
[19] Hung P K, Vinh L T, Nghiep D M and Nguyen P N 2006 *J. Phys.: Condens. Matter* **18** 9309
[20] Huang C and Cormack A N 1992 *7th Int. Conf. Cambridge (London, Washington, DC Aug. 1991)*; *Phys. Non-Cryst. Solids* 31
[21] Hoang V V and Oh S K 2005 *Physica* B **364** 225
[22] Taraskin S, Elliott S and Klinger M 1995 *J. Non-Cryst. Solids* **192/193** 263
[23] Chan S L and Elliott S R 1991 *Phys. Rev.* B **43** 4423
[24] van Beest B W H, Kramer G L and van Santen R A 1990 *Phys. Rev. Lett.* **64** 1955
[25] Mozzi R L and Warren B E 1969 *J. Appl. Crystallogr.* **2** 164
Mozzi R L and Warren B E 1970 *J. Appl. Crystallogr.* **3** 251
[26] Pettifer R F, Dupree R, Farnan I and Sternberg U 1988 *J. Non-Cryst. Solids* **106** 408
[27] Benoit M and Kob W 2002 *Europhys. Lett.* **60** 269
[28] Trave A, Tangney P, Scandolo S, Pasquarello A and Roberto C 2002 *Phys. Rev. Lett.* **89** 245504
[29] Barrat J L *et al* 1997 *J. Comput. Simul.* **20** 17
[30] Mozzi R L and Warren B E 1969 *J. Appl. Crystallogr.* **2** 164
[31] Grimley D I, Wright A C and Sinclair R N 1990 *J. Non-Cryst. Solids* **119** 49
[32] Konnert J H and Karle J 1973 *Acta Crystallogr.* A **29** 702
[33] Hoang V V *et al* 2007 *J. Phys.: Condens. Matter* **19** 116104
[34] Hoang V V 2006 *Eur. Phys. J.* B **54** 291
[35] Stixrude L and Bukowinski M S T 1989 *Geophys. Res. Lett.* **16** 1403